Pollution 2022, 8(4): 1233-1249
DOI: 10.22059/POLL.2022.341201.1430

RESEARCH PAPER

Effect of adding Arabic Gum and Zinc Oxide Nanoparticles to MBR Membranes Supported by Carbon Nanotubes for Ultrafiltration Process of Dairy Wastewater

Mohammed A. Abdul-Majeed[1], Amer N. Al-Naemi[1], Mustafa H. Al-Furaiji[1,*], Inmar N. Ghazi [2]

[1] Ministry of Science and Technology, Environment and Water Directorate, Baghdad- Iraq
[2] Communications Engineering Department, University of Technology/ Baghdad-Iraq

Received: 05.04.2022, Revised: 15.06.2022, Accepted: 20.07.2022

Abstract
There is great competition to improve the performance of membranes for water treatment within the scope of the research, especially the problem of biofouling on the membrane as it is related to the performance and life of the membrane. This study introduces a new mixture of hybrid bioreactor membranes that combine oxidized multi-walled carbon nanotubes (OMWCNTs) with polyethersulfone (PES) using a phase inversion method, along with equal proportions of zinc oxide nanoparticles (ZnO NPs) and Arabic gum (AG) from an acacia tree, for application in a submerged membrane bioreactor to treat wastewater for a dairy product at the College of Agriculture / Baghdad University. The results when comparing the nascent composite membranes (PES / OMWCNTs / ZnO / AG) with that of (PES / OMWCNTs) indicated that the membrane mixed with ZnO / AG has more hydrophilicity(16%) As well as reducing the negative charge on the surface of the membrane almost three times, As evidenced by the water contact angle test and the zeta potential data respectively, furthermore, the atomic force microscopy analysis showed that this improved membrane showed lower values of surface roughness (by 46.8%), and more flexible normal flux values (by almost doubling), Moreover, the rate of rejection increased when the bovine serum albumin (BSA) solution was passed a percentage (13%) when compared with PES / MWCNTs membrane. Importantly, the prepared membrane also presented removal efficiency of chemical oxygen demand (COD) was significantly 37.5%higher when compared with the commercial MBR system.

Keywords: Wastewater treatment; Water flux; Fouling; Polyethersulfone membranes

INTRODUCTION

The water treatment process is considered one of the most important aspects of providing water sources, especially in arid and semi-arid areas (Waisi et al., 2015). Industrial water treatment is a process used for a range of applications with simple, complex, efficient, and low-cost systems to handle various water purification and separation needs (https://www.sciencedirect.com/science/article/abs/pii/S2589014X21000578 - !Alalwan et al., 2021a; Kadhom et al., 2019a). A membrane bioreactor (MBR) for water treatment is a purified wastewater treatment process that combines biological water treatment and membrane filtration (Dixon et al., 2020; Abaas et al., 2012). This innovative technology offers many advantages over the traditional treatments of activated sludge, including the increase in the high biomass concentration, the disposal of the sedimentation unit in addition to the improved water quality resulting from the treatment.

* Corresponding author Email: alfuraiji79@gmail.com

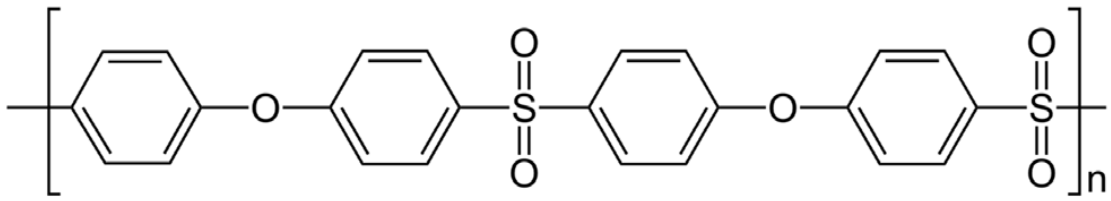

Fig 1. Molecular Structure of Polyethersulfone Molecular Formula $(C_{12}H_8O_3S)_n$

Nano-membrane production technology is one of the most widely used technologies in today's industrial sectors (Nisreen et al., 2022; Kadhom et al., 2016), with broad applications in water treatment, food, pharmaceutical, oil, gas and power industries. Although the membranes are efficient in treating polluted water, they face some problems.The most critical problem faced by membrane technology is the deposition of colloids, particles, large particles, salts, and others on the walls of pores, inside the pores, or the surface of the membrane, thus reducing the efficiency and life of the membrane. Controlling sediments is an essential step for membranes to be competitive compared to other technologies, and this is done by choosing the type of polymeric material used in preparing the membranes (Jing et al., 2020). Polyethersulfone (PES), Figure 1 has the highest values of temperature resistance and tensile modulus in elasticity. PES properties are similar to those of polysulfone (PSU), although it exhibits a higher impact strength and better chemical resistance. Its stiffness and stability are high, and its notch sensitivity is low (Weibin et al., 2020).

PES membrane had more efficient salt rejection and better antifouling properties. (Mansourpanah et al., 2011) prepared polycaprolactone-modified multiwalled carbon nanotubes (PCL-MWCNTs) to fabricate PES/PCL-MWCNTs nanocomposite membranes. The results indicated that the porosity of nanocomposite membranes was increased, and the fouling tendency declined. Carbon nanotubes (CNTs) and other nanomaterials have proven their importance and have wide applications in many fields (https://www.sciencedirect.com/science/article/abs/pii/S2589014X21000578 - !Alalwan et al., 2021b; Malik et al., 2021 and Kadhom et al., 2019b).

Carbon nanotubes have attracted much attention because of their unique combination of rigidity, strength, and lightweight, with excellent chemical and mechanical properties, so it has been used as a filler to develop water treatment membranes (Celik et al., 2011). Carbon nanotubes are nanoparticles in the form of nanometer-sized tubes and consist of a huge array of hexagonal structures that are made up of carbon atoms.

Carbon nanotubes (CNTs) have proven useful in many applications including biomedicine, energy storage, sensors, and electronic devices. Kalra and his colleagues (Kalra et al., 2003) have been able to transport water molecules that are osmotically driven through carbon nanotubes, proposing an exciting opportunity to use networks of nanotubes and assemblies to efficiently purify water. Afterward, several studies were carried out to incorporate carbon nanotubes with polymer materials to prepare an advanced membrane for water treatment. One of these studies (Ma et al., 2010) produced a new sort of high permeability nanofibers containing OMWCNTs integrated into the polyvinyl alcohol barrier layer (PVA), the improved flux of water is due to the emergence of multi-directional water channels through the strong bonding between the exact microfiber nanotubes themselves and the connection between the filler and the barrier layer matrix.

Recently, inorganic nanoparticles (NPs) such as zinc oxide nanoparticles (ZnO) and multi-walled carbon nanotubes (Narang et al., 2018) have been combined to improve the permeability due to the unique one-dimensional structure of the carbon nanotubes and their superior mechanical and chemical properties, It has been used as fillers for numbers of the flat membrane

and current research is still attempting to achieve homogeneous dispersion of MWCNTs and compatibility with polymer matrix through strong interactions.

Also, Arabic gum from the acacia tree is considered a hydrophilic and bio-absorbent material to remove toxic mineral pollutants from aqueous environments. It is also used as a binder and is environmentally friendly to achieve stability when adding nanoparticles to the matrix of membranes when manufacturing (Jiang et al., 2018).

Current research has shown that to successfully obtain a sophisticated CNT / polymer nanocomposite, homogeneous dispersion of carbon nanotubes within the polymer matrix has to be achieved through strong interfacial interactions (Hossein et al., 2018). As a result, several applied studies have been carried out to improve the dispersion of carbon nanotubes and their compatibility with the polymer matrix through various chemical or physical modifications. One of these methods is an acidic treatment (Reyhan et al. 2018), where the carboxyl and hydroxyl groups are concentrated on the edges of the carbon nanotubes and at the fault sites, which makes those extra efficient and thus the best dispersion (Ahmad et al. 2019).

The main purpose of this study is to prepare an MBR membrane for industrial wastewater treatment.The phase inversion method was used to prepare flat sheet membranes with the addition of multi-functional oxidized carbon nanotubes and zinc oxide nanomaterials with reinforcement by adding Arabic gum from the acacia tree, which has the advantage of being a hydrophilic and environmentally friendly binder.

MATERIALS AND METHOD

Polyethersulfone granule, 3 mm nominal granule size, zinc acetate ($Zn(CH_3COO)_2 \times 2H_2O$), polyvinylpyrrolidone (PVP; K-30), sodium dodecyl sulfate (SDS), and 1-Methyl-2-pyrrolidinone (NMP, 99.5%) were purchased from Sigma Aldrich, No purification was carried out on the chemicals purchased. Multi-walled carbon nanotubes (MWNTs, >95%, OD 5-15 nm, ID 3-5 nm, length ~50μm, and purity of 95%) were manufactured by US Research Nanomaterials Inc., USA. White Acacia gum powder (Viscosity; 70-110 Mpsc) was purchased from Mumbai, India.Oxalic acid dehydrate [$H_2C_2O_4 \cdot 2H_2O$], absolute ethanol (99%), and diethylene glycol were analytical grade and purchased from Merck.

MWCNTs were functionalized according to previous work (Abdul-Majeed et al., 2022) briefly, by adding it to a pre-prepared acid solution consisting of mixed (H_2SO_4 / HNO_3 = 3/1 in volume), whereas the organic solvents lead to increased dispersion. 1 g of MWCNTs powder was added to 100 ml of the acid mixture and refluxed at 80-100 °C for 3.5 hours as shown in Figure 2. After the reflux process was complete, the dispersion of the carbon nanotubes in the acid mixture was increased using a 70 °C ultrasound for 6 hours. Then they were left overnight to dry at room temperature after being washed with DI. In the final step, a 0.2 μm polymer filter was used to filter the carbon nanotubes with washing until the pH of the MWCNTs solution was 7.0 ± 0.2 as shown in Figure 2. The nanotubes were dried again in an oven at 100 °C overnight to obtain oxidized carbon nanotubes (OMWCNTs).

The surface structure and morphology of the carbon nanotubes are described by electron microscopy (SEM, VEGA3 - TESCAN, Czechoslovakia). The SEM sample was prepared by blending ethanol-carbon nanoparticles and dropping them onto the silicon wafer. Allow the sample to dry thoroughly at room temperature, and then wrap the paste with a spherical layer of goldInfrared spectroscopy (FTIR; IRPrestige-21, SHIMADZU, Japan).

It is essential to prevent the accumulation of OMWCNTs, as they were dispersed using ultrasound after mixing a certain amount of them in a glass flask with 25 mL of an aqueous surfactant solution SDS which is easy to chemical absorption on the surface of the carbon nanotubes because it leads to electrostatic repulsion that prevents the accumulation of carbon tubes together. The nanocomposite material OMWCNT/ZnO was prepared by the sol-gel

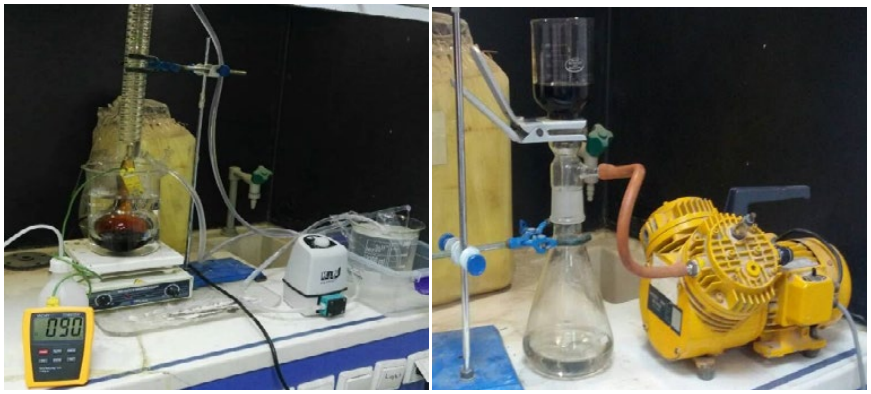

Fig 2. Preparation of the oxidized MWCNTs.

method. Initially, the precursorsolutions were prepared, which were a mixture of oxalic acid (Oxa) and zinc acetate (Zia) in ethanol at 0.15:0.1M, respectively and separately. Zinc acetate was dissolved with ethanol and heated to 60 °C for 30 minutes and then a certain amount of diethylene glycol was added to it which worked as a surfactant. The ethanol oxalic acid solution was heated to 50 °C and then this solution was added dropwise and gently to a zinc acetate solution at a ratio of (Zia/Oxa) was (40/ 60); a constant amount of OMWCNT was added to Zia / Oxa sol. The mixture was mixed with ultrasound for 1 hour for optimal dispersion of MWCNTs. The mixture was then heated at 180 °C with continuous stirring at 150 rpm for 3 hours. Finally, the solution is allowed to cool in a dark place at room temperature. Then it was washed with ethanol and deionized water many times and then dried at 120 °C for 7 hours. Two composite flat sheet membranes (CFSM) were prepared. Initially, the OMWCNTs, PES,and PVP were dried in an oven for 2h at 50°C.In the first membrane,the casting solution was prepared by dissolving PES/PVP in NMP separately (Abu-Dalo, et al., 2022), with a concentration of 17 wt. %PES and 5 wt. % PVP (was used as a pore maker), then the mixture was placed in a water bath and heated to a temperature of 55-60° C, with a stirring rate of 500 rpm using a magnetic stirrer until a homogeneous mixture is obtained. In another flask, a certain amount of OMWCNTs is dissolved in a certain amount of solvent NMP at room temperature, the solution OMWCNTs/NMP mix well using ultrasonic then added to a solution of PES/PVP with a constant stirring of the mixture at 60 °C for a period of not less than 7 hours. A dope solution containing PES / PVP has been modified with the addition of OMWCNTs at a concentration of 2.5 wt% relatives to PES this percentage was the best through tests that we conducted in previous work (Abdul-Majeed et al., 2022).The second composite membrane was prepared by repeating the same steps as preparing the first membrane. However, the nanocomposite includes dissolving ZnO / OMWCNTs in NMP at room temperature for 20 hours, dissolving AG in NMP at a ratio of (1/12) at 60 °C for 20 hours with continuous stirring, and then dispersing by ultrasound for 1 hour (Ahmad et al., 2019). The solutions were then mixed with vigorous stirring for 1 hour at room temperature. Then the gases were expelled using ultrasound for 2 hours at room temperature (Ahmad et al., 2019). The composition of the casting solutions and the content is detailed in Table (1). The homogeneous pouring solution was kept stagnant in a dark place for at least 24 hours to allow air bubbles to come out to prevent defects in the membrane. Afterward, some of the polymeric casting solutionswere cast on a clean glass plate and dispersed using a motorized film applicator CX-4 (Germany), in the thickness of 150 μm. As shown in Figure 3, after a 15s evaporation time of the casting solution, the glass is submerged in a bath of deionized water at room temperature to induce the phase inversion process.The membrane was thoroughly rinsed with deionized water to remove residual solvents in the formed membranes.

Finally, the prepared membrane was stored at room temperature in deionized water

Table 1. The compositions of casting solution used in this study (mass %)

	CFSM-1	CFSM-2
PES(%)	17	17
PVP (%)	5	5
OMWCNTs(%)	0.5	0
OMWCNTs/ *ZnO* (%)	0	0.5
Arabic Gum (AG)	0	0.5

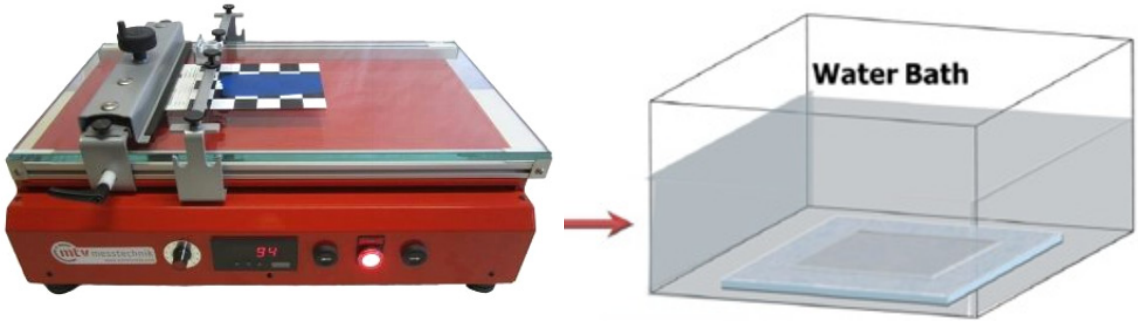

Fig 3. Phase inversion process for composite membranes fabrication using the motorized film applicator CX-4 (Germany)

containing formaldehyde at a concentration of 1 wt% to keep the membrane from growing bacteria.The nascent membranes were then verified using a scanning electron microscope (SEM, VEGA3 - TESCAN, Czechoslovakia),and the wettability of membranes was studied by measuring the contact angle using (Theta Lite TL-101 Thailand), this indicates the degree of moisture when contacting a solid and liquid.Contact angles (less than 90 degrees) indicate high wetness (hydrophilic), while contact angles (>> 90 degrees) indicate low wetness (hydrophobic), (Chandrashekhar et al., 2019).

Performances of prepared composite membranes were characterized by measuring the water flux of pure water and the rejection of bovine serum albumin protein (BSA). A feed solution of BSA with a concentration of 1 g / l was used at pH 7.0 ± 0.2 as a typical organic substance. The flux of membranes fabricated was tested at room temperature and pressure of 2 bars with the laboratory-scale dead-end filtration (Sterlitech Corporation HP 4750: Figure 4) after compaction at 3 bars for 30 min to get a steady flux.The effective area of the dead-end filtration system was 14.6 cm^2. Compressed air was used to provide the necessary pressure driving force to feed flow across the membrane. A magnetic stirring gadget is placed over the position of the membrane in the filter cell with a clogged end to reduce the effect of polarizing on the flux and stirring the flipping continuously.

The membrane flux (J) was measured bypassing pure wateror BSA through them at 2 bars by recording the volume of permeation water & BSA for a 130 minutes filtration period. The calculation of the different membrane fluxes was performed as follows:

$$J = \frac{V}{At} \tag{1}$$

Where J is the flux of pure water (l/m^2 h), V the permeate volume (l), A the membrane area (m^2) and t is the time (h).

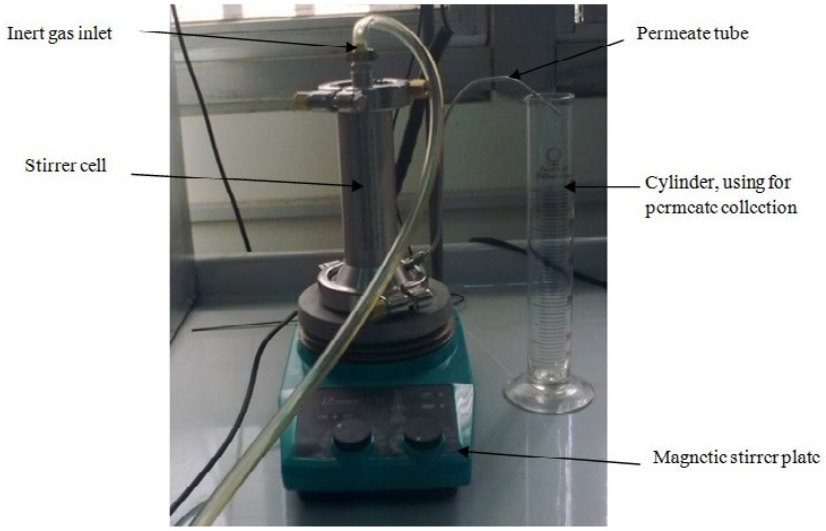

Fig 4. Photograph of the dead-end filtration cell (STERLITECH HP4750)

Membrane porosity ε (%) was defined as the volume of the pores divided by the total volume of the porous membrane. It could usually be determined by the gravimetric method, the porosity of the membranes was tested according to the method provided earlier by (Yalei et. al., 2014).

$$\varepsilon = \frac{\left(w_{wet} - w_{dry}\right)/\rho_w}{\left(w_{wet} - w_{dry}\right)/\rho_w + w_{dry}/\rho_p} * 100\% \quad (2)$$

Where:

w_{wet} the weight of the wet membrane (g).

w_{dry} the weight of the dry membrane (g).

ρ_w the pure water density (0.998 g/cm^3).

ρ_p the polymer density (as the inorganic content in the membrane matrix was small and ρ_p was approximate to ρ_{PVDF}, namely 1.765 g/cm^3).

The aqueous solution BSA was used to characterize the rejection. The UV / Vis spectrophotometer (SPEC ORD 200 PLUS/Analytik Jena AG, Germany) was used to determine the BSA concentration in feed and permeate samples along the 280 nm wavelength (Chandrashekhar et al., 2019) the rejection calculation formula is shown below:

$$R = \left(1 - \frac{C_p}{C_f}\right) \times 100\% \quad (3)$$

Where $C_p and\, C_f$ are the permeate concentrate and the feed concentrate of BSA, respectively. To minimize experimental error, the filtration experiment was repeated three times to obtain the average. And standard deviations were reported as error bars.

The performance of the modified membranes was tested in the MBR system from Ecologix Technologies Asia, Taiwan. More details on the MBR system can be found elsewhere (Dixon et al., 2020). The submerged UF membranes retain all solids, bacteria, and germs bigger than approx. 0.04μm separation size and guarantee maximum effluent quality. The membrane filtration system, along with all ancillary equipment, is shown in Figure 5.

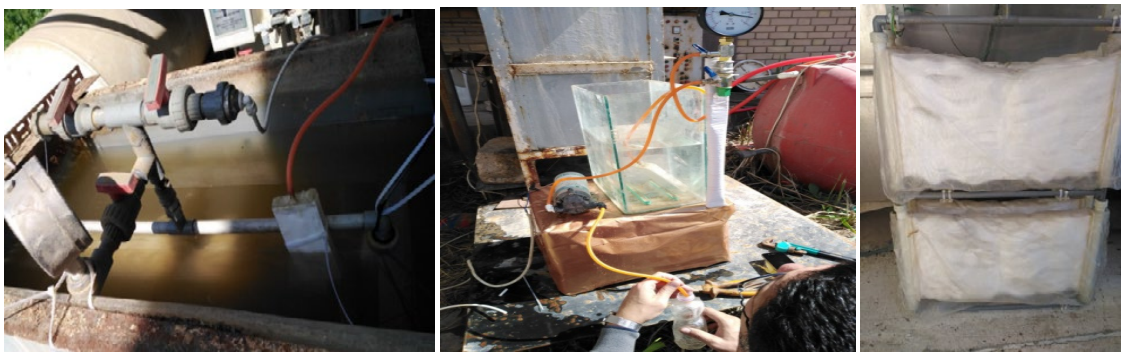

Fig 5. Our membrane operates within the MBR system of the Dairy factory of the College of Agriculture.

RESULTS AND DISCUSSION

SEM images showed that raw MWCNTs shown in Figure 6-a contained bulk materials that may be impurities and metal catalysts. After the acid oxidation process, impurities and metal catalysts in OMCWNT, Figure 6-b were largely absent, these images were consistent with (Jun et al., 2013). The OMWCNTs were combined in a matrix with ZnO NPs, where the SEM micrographs of the OMWCNTs/ZnO/AG show in Figure 6-c the formation of a coarse white microstructure that decorates the carbon nanotubes and is highly porous conducive to the adequate fixation of Arabic gum with the polymeric structure of the membrane. These results are consistent with what both reported (Zinadini et al., 2017) and (Ahmad et al., 2019).

Scanning electron microscopy images of the surfaces of the composite membranes are shown in Figure 7. Both membranes show a homogeneous distribution of the interstitial bond between OMWCNTs and their presence within the pores within the polymer matrix. The image gives the impression that the membrane is in the form of a sponge-like layer or a layer of skin over a porous infrastructure due to the solvent removal process by phase reflection. There are a good number of well-distributed pores in the surface layer of the membrane. This is helped by the presence of PVP inside the polymer matrix, which provided bonding between the carbon nanotubes and the PES matrix as shown in Figure 7, we also note the high and efficient dispersion of the carbon nanotubes, the explanation for this is that during sonication, SDS helps to exfoliate and disperse the carbon nanotubes, as the SDS particles were absorbed on the surface of the carbon nanotubes and their accumulation was prevented by electrostatic repulsion.

The morphology of the second complex membrane (CFSM-2) is shown in Figure 7, in this image it can be seen that the OMWCNT is completely covered as a result of the growth of the ZnO nanostructure on the surface of the OMWCNT. It is interesting that important visible changes in surface morphology can be seen, including an increase in surface porosity due to the addition of ZnO and AG within the membrane structure due to the fact that the hydrophilic affinity for these materials enhanced the rate of mass transfer between the solvent and the non-solvent during the coagulation process, and thus lead to the creation of larger porous channels (Alhoshan et al., 2013). Comparedto the surface membrane sample (CFSM-1). The additions to both membranes did not cause any perturbation affecting the structural integrity of the membrane surface.

Figure 8 and Figure 9 show the FT-IR spectra of composite membranes CFSM-1 & CFSM-2 respectively, where the peak at 1575.84 cm^{-1} may be due to the vibration of the carbon structure of the CNTs. As shown peaks have appeared around 1313.52 and 3433.92 & 3444.87 cm^{-1} after the acidic oxidation process these are corresponding to C-C-O, C-O, and -OH extending in carboxyl groups (-COOH), sequentially (Jiang et al. 2009). The presence of these changes is

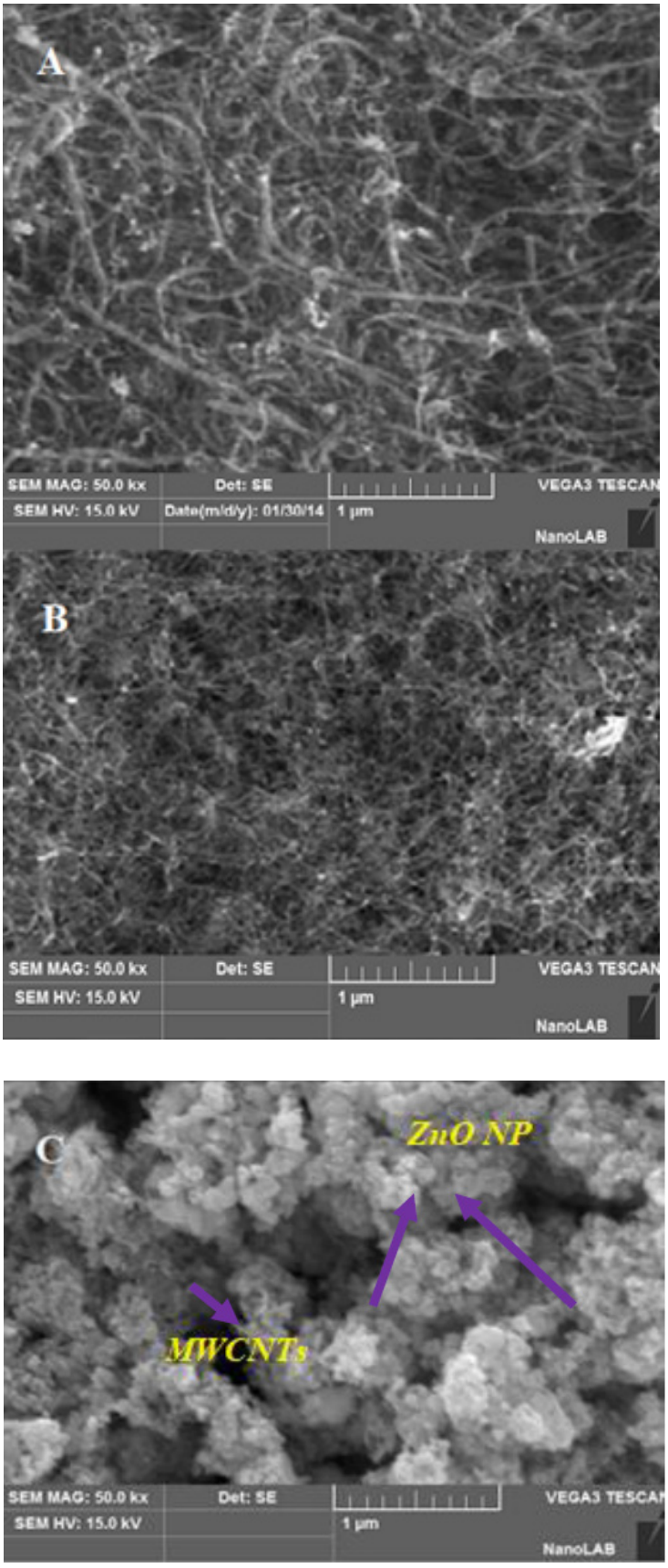

Fig 6. SEM imeges: (a) raw MWCNTs (b) oxidized MWCNTsand (c) OMWCNTs/ZnO/ AG

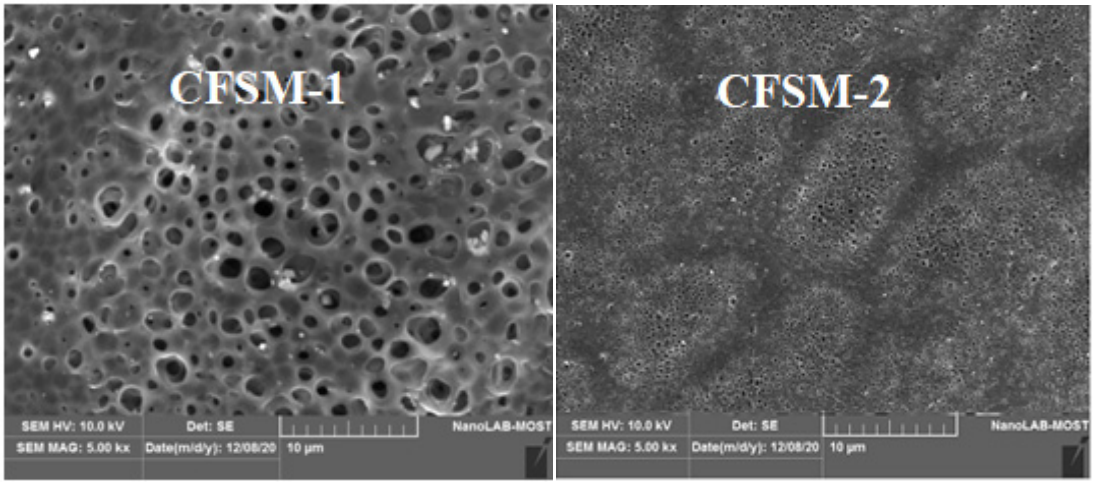

Fig 7. SEM images of composite flat sheet membranes with and without the nanomaterials.

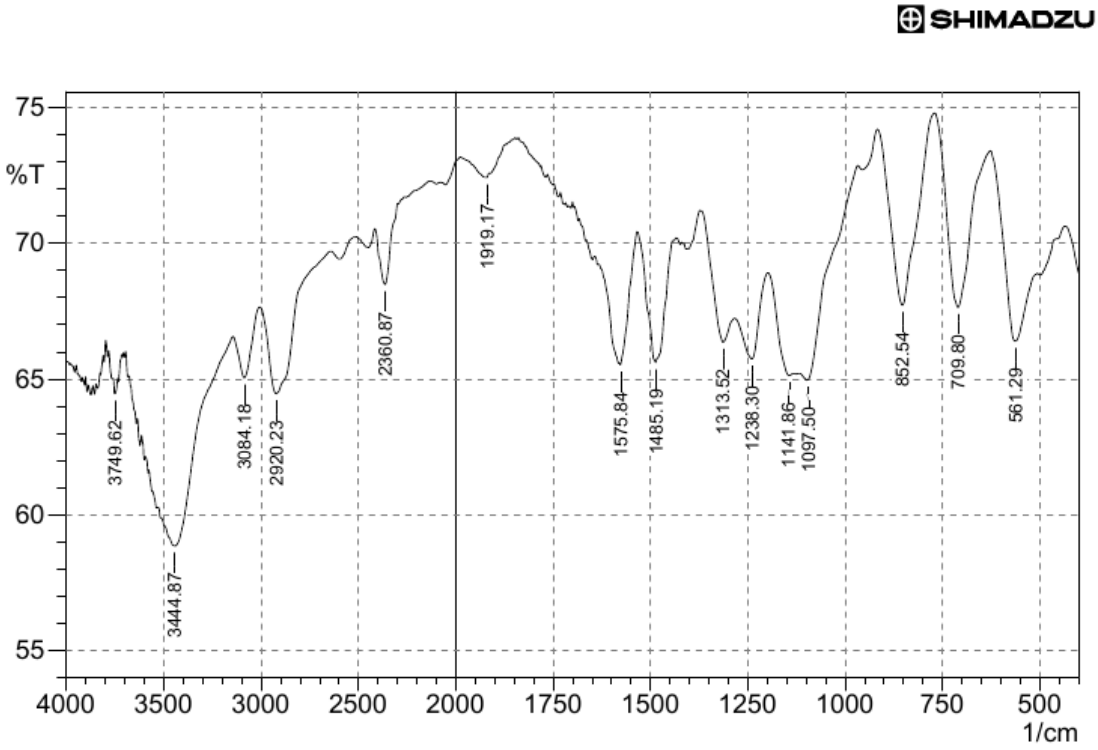

Fig 8. FTIR spectra of CFSM-1

supported by the success of the oxidation process of CNTs. The two bands have appeared around 2360.87 and 2362.80 cm^{-1} these can be attributed to the C=C double bonds stretch vibration, which originated from the surface of carbon nanotubes. While the infrared spectra of ZnO / OMWNTs nanocomposites resulting from surface chemistry show us the difference between the OMWCNTs and OMWNTs/ZnO nanocomposites. Two other weak peaks can be seen around 1656.58 cm^{-1} and 3853.77 cm^{-1} (Alminshid et al., 2021), which can be assigned to the stretching vibrations of OH groups. Compared with the infrared spectra of OMWCNTs, the peak at 2,362.80 cm^{-1} is narrower and has an area of 10.968 while the corresponding peak at 2360.87 cm^{-1} has

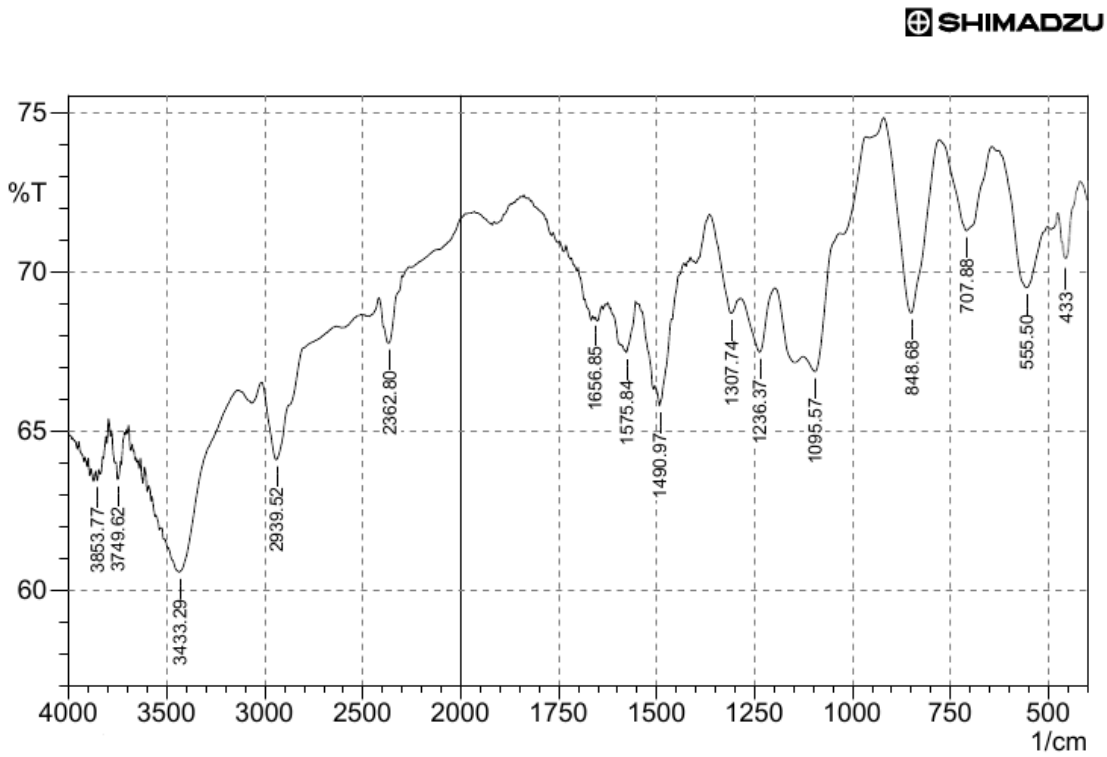

Fig 9. FTIR spectra of CFSM-2

Table 2. The root mean square (RMS) of fabricated membranes

Membrane	RMS
CFSM-1	7.05±1.025
CFSM-2	4.8±0.804

an area of 17,855 and the two bands around 1919.17, 1575.84 cm^{-1} It is lower in the composite membrane CFSM-2 than in the composite membrane CFSM-1. The results concluded that the surface of MWCNTs has been nearly coated at the surface active sites by ZnO NP. Evidence for this is the peak observed at about 433 cm^{-1} in Figure 9 dedicated to the presence of ZnO NP. In addition, the FT-IR spectra show the presence of Arabic gum through the presence of an additional wide wave at 3853.77 cm^{-1} attributable to the OH functional groups normally present in carbohydrates (such as starch, cellulose, or glycogen) whose molecules consist of a number of sugar molecules bound together and also attributed to the vibration of N-H in amines. These results are consistent with what was previously reported (Eman et al., 2016).

Figure 10 & Figure 11 show the atomic force microscopy (AFM) images of the two composite membranes (CFSM-1 & CFSM-2), where we note the presence of chains with luminous golden peaks that represent the tops of the membrane surface. Indeed, the dark areas indicate valleys and low areas. These pictures show the apparent difference in the surface roughness, as the membrane grafted with (ZnO/AG) has the root mean square (RMS) roughness is much less valuable than the membrane not grafted with these materials, as shown in Table (2). These results are in line with other research. Significantly higher roughness values have been reported for virgin membranes than for composite or hybrid membranes. This result corresponds to the shape of the smooth surface that was seen using a scanning electron microscope, and the reason

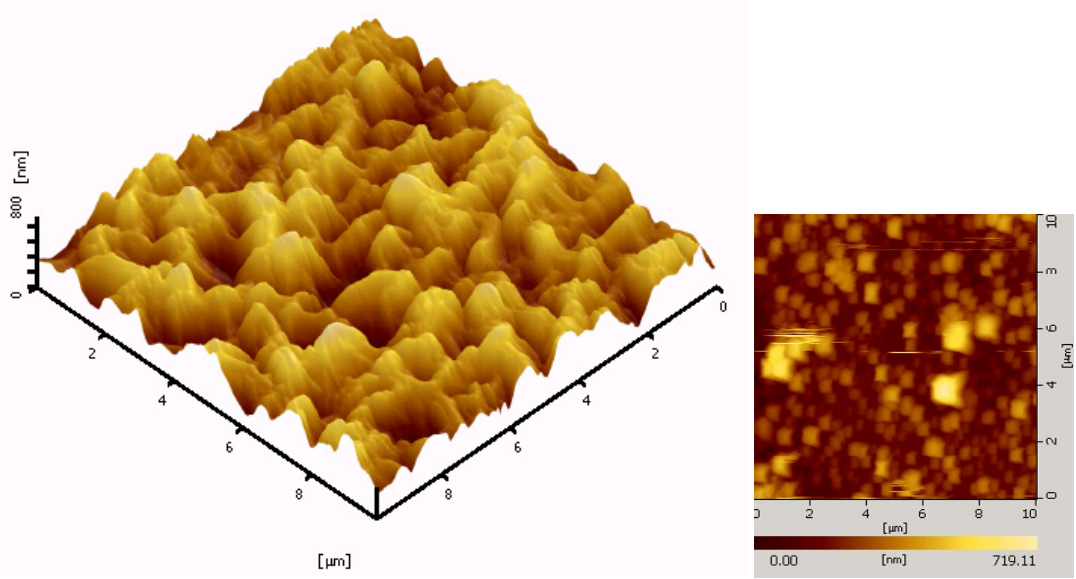

Fig 10. AFM images of composite flat sheet membrane (CFSM-1)

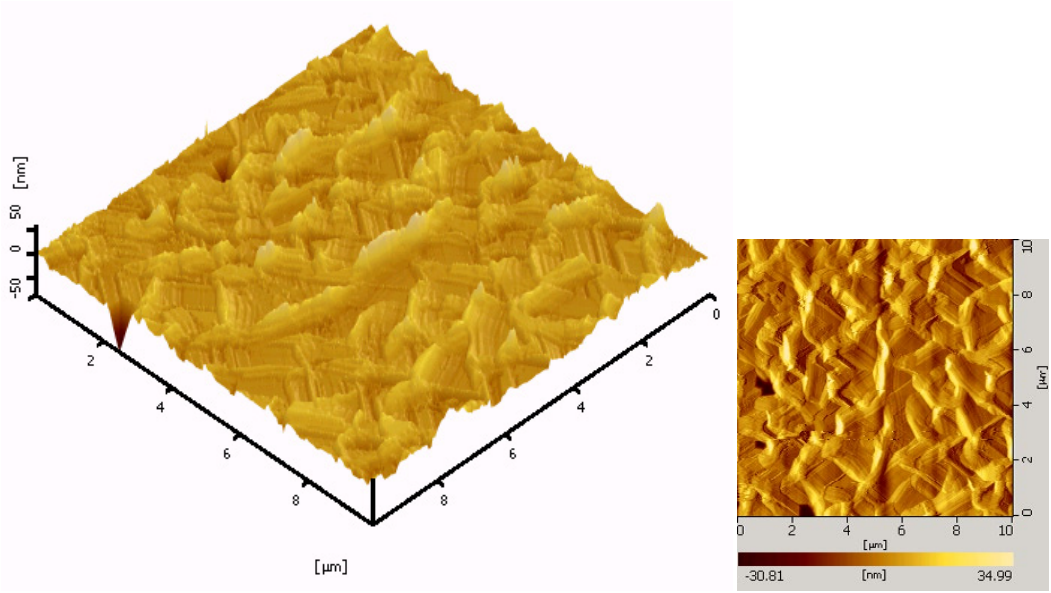

Fig 11. AFM images of composite flat sheet membrane (CFSM-2)

for the surface to appear smoother was due to changes in the viscosity of the casting solution when adding fillings, which were in harmony with the membrane matrix, and did not cause a change in the structure of the membrane and did not cause a high electrostatic interaction between them. These results are close to what was previously reported by (Zinadini et al., 2017) and (Ahmad et al., 2019).

Contact angle decreased from about 56.4° for composite membrane CFSM-1 to 48.6° for CFSM-2 as shown in Figure 12, where the percentage improvement in hydrophilicity can be calculated and is about 16%. This conclusion has been listed by (Choi et al., 2007) and is associated with the fact that through the phase inversion process, the hydrophilic OMWCNTs/ZnO/AG was engaged with pores at the membrane surface. The low contact angle indicated that ZnO/

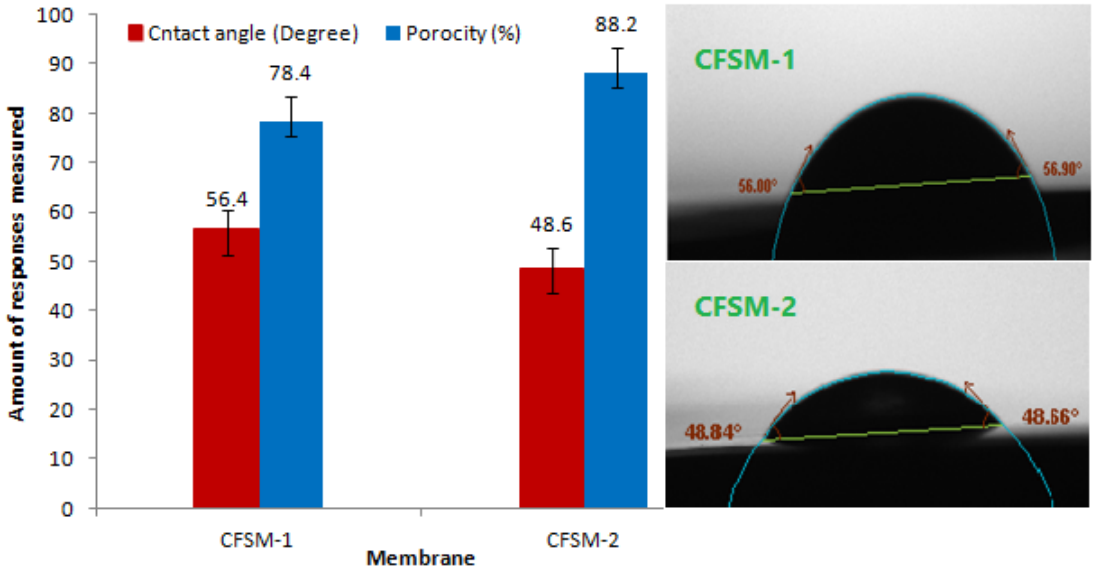

Fig 12. Static water contact angle and porosity of the composite membranes

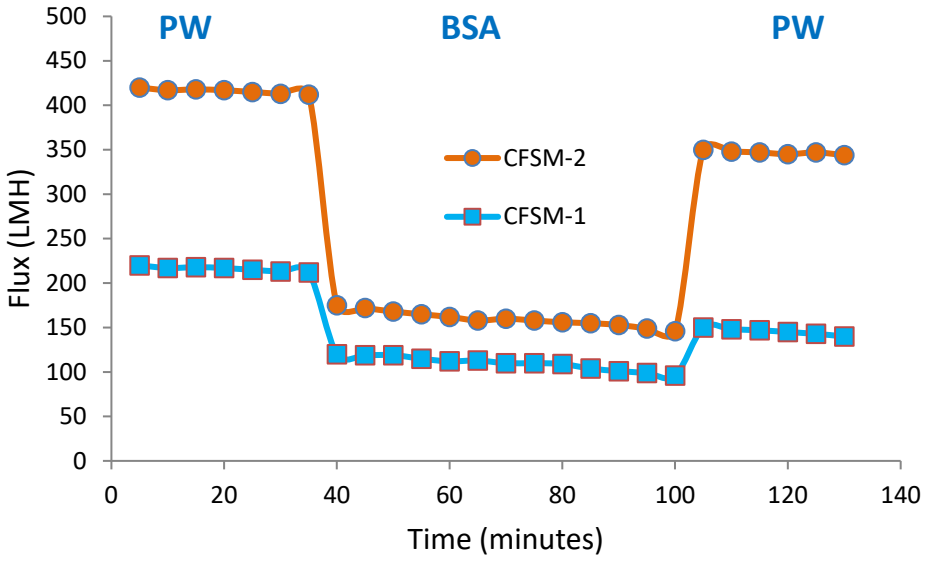

Fig 13. Fouling behavior of prepared membranes with filtration of DW &BSA solution (1000 mg/L, pH~7.4)

AG combined with the PES/MWCNTs membrane could improve wet ability, thereby reducing membrane contamination caused by organic matter proteins. The porosity of the dense PES membranes was improved by adding a small number of modified MWCNTs. This result can be attributed to the presence of hydrophilic MWCNTs in the polymeric matrix resulting in a rapid exchange of solvent and non-solvent in the phase inversion process (Lalia et al., 2013), and upon reinforcement with ZnO NP in addition to a percentage of Arabic gam, the result was impressive. These results are close to what was previously reported (Ahmad et al., 2019).

Results related to flux and biofouling resistance of the fabricated membranes were as shown in Figure 13, where the flux was shown in different stages, where the membrane sample CFSM-2 showed a superior initial pure waterflux. The flux increased by twice as much as compared to the CFSM-1 membrane's initial flow with pure water. This massive flux improvement was expected

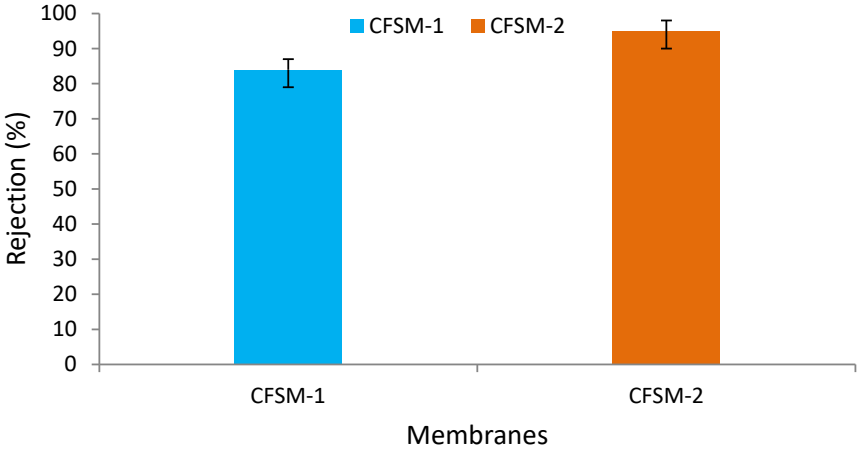

Fig 14. BSA rejection of different fabricated membranes.

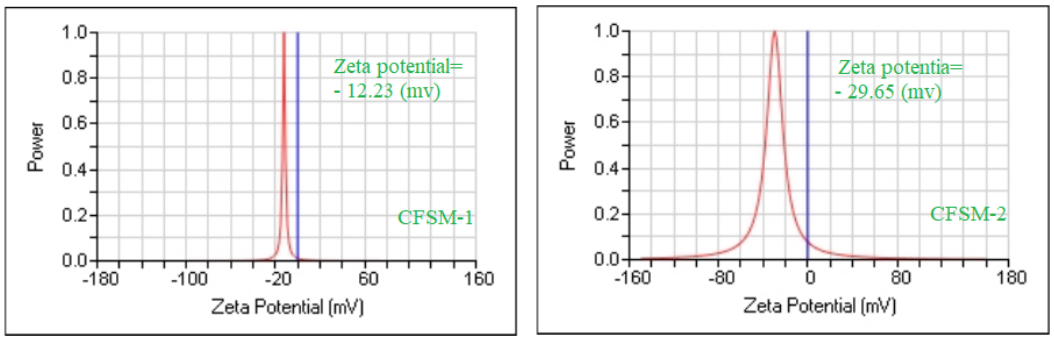

Fig 15. Zeta potential data for fabricated membranes (CFSM-1 and CFSM-2).

as it stands to reason that more hydrophilic and higher porosity membranes would have higher flux. Upon filtering of 1000 ppm of BSA, all membranes indicated a gradual decrease in fluxes over time due to the BSA adsorption on the membrane surface and the creation of the cake layer during the permeation of the protein solution. However, the CFSM-2 sample with less surface roughness showed much higher flux recovery than the CFSM-1 membrane. This is explained because the enhanced flux attributed to increased water porosity and surface charge improves flux recovery performance. This is what the composite membranes have shown, Direct proportionality, i.e. the preference of the membrane after adding ZnO and AG. Additionally, when returning to passing pure water through the membrane again, the flux improves for the composite membranes, but the preference remains for the CFSM-2 membrane. These results appear to be very consistent with his finding (Ahmad et al., 2019).

The rejection data for 1000 ppm of BSA solution for different membranes are shown in Figure 14. The results showed that the effect of adding zinc oxide nanoparticles and Arabic gum leads to improving the rejection of the membrane by grafting the composite polymeric membrane of oxidized carbon nanotubes with these materials. This can be explained by the fact that these nanoparticles settle in the pores and thus reduce the size of the pores and increase the rate of rejection, despite the fact that they increase the overall porosity of the membrane and thus improve the rejection of organic materials and pollutants and this is an important requirement in the performance of membrane bioreactor (MBR) to treat wastewater from dairy products. These results appear to be consistent with his finding (Ahmad et al., 2019).

Revealed zeta data are shown in Figure 15 for the manufactured membranes. It is noted that the two membranes (CFSM-1 & CFSM-2) have a negative charge, but the negative charge

Table 3. Comparison of the prepared membrane with the commercial MBR system.

Tests	Dairy wastewater	Commercial MBR	Processed water by CFSM-2	National Determinants of Drained Water (449) of 2012
BOD_5	400-1500 mg/l	10 mg/l	3-5 mg/l	10 mg/l
COD	750-2000 mg/l	30-55 mg/l	10-40 mg/l	40 mg/l
NO_3-N	200-250	20-50 mg/l	10-30 mg/l	50 mg/l
PO_4-P	6-10 mg/l	5-10 mg/l	1-2 mg/l	12 mg/l
TOC	100-150 mg/l	10-25 mg/l	5-15 mg/l	
Turbidity	100-200 NTU	1-5 NTU	1 NTU	-
pH	3-5.5	7.2-8	7.2-8	6-8

increases when both nano zinc oxide and Arabic gum are added at neutral pH. The increase in the negative surface charge of the composite membrane CFSM-2 compared to the CFSM-1 membrane samples can be explained by the presence of hydrophilic residues of AG, which contain the carboxylic groups as well as the hydrophilic functional groups present on ZnO NP and OMWCNTs.

The prepared membranes were tested in a pilot-plant MBR system installed at the dairy factory, College of the Agriculture / University of Baghdad. Table (3) shows the characteristics analysis of the dairy wastewater before and after treatment with the commercial MBR system and our synthesized membrane (i.e. CFSM-2). The results showed that CFSM-2 membranes revealed a better or similar performance to the commercial MBR system in treating real dairy wastewater. Also, the quality of the treated water was within the limits of the discharged water quality.

CONCLUSION

Incorporation of a compound membrane PES with MWCNTs along with equal proportions of zinc oxide nanoparticles and Arabic gum from an acacia tree for application in a submerged MBR for dairy water treatment successfully prepared through a phase inversion process. A comparison was made with the composite membrane (PES/MWCNTs) without nano-zinc oxide and AG. This study demonstrated that flat plate membranes containing OMWCNTs / ZnO / AG could be synthesized after oxidation and activation of carbon MWCNTs in mixed concentrated acid. The results showed that the effect of adding zinc oxide nanoparticles and Arabic gum leads to improving the performance of the membrane by grafting the composite polymeric membrane to the carbon nanotubes to be oxidized with these materials. Incorporation of ZnO / AG into the membrane matrix grafted with oxidized carbon tubes resulted in the color of the membrane from dark gray to uniform white. The enhanced membrane is characterized by a low contact angle and high porosity compared to the membrane containing only carbon nanotubes, indicating the improvement of the hydrophilic membrane. The results showed that when testing the flow and rejection using pure water and BSA solution, the grafted membrane was better than the membrane without these substances. In addition, the new membrane was shown to enhance the resistance to protein contamination of the films after being tested with a 1000 ppm of BSA solution.

ACKNOWLEDGMENT

The authors gratefully acknowledge the scientific support of the Environment and Water Directorate, Ministry of Science and Technology, Baghdad, Iraq.

GRANT SUPPORT DETAILS

The present research did not receive any financial support.

CONFLICT OF INTEREST

The authors declare that there is not any conflict of interests regarding the publication of this manuscript. In addition, the ethical issues, including plagiarism, informed consent, misconduct, data fabrication and/ or falsification, double publication and/or submission, and redundancy has been completely observed by the authors.

LIFE SCIENCE REPORTING

No life science threat was practiced in this research.

REFERENCES

Abbas, T. R., Abdul-Majeed, M. A. and Inmar, N. Ghazi. (2012). Testing the Applicability of Submerged Hollow Fiber Membrane Bioreactor (MBR) Technology for Municipal Wastewater Treatment in Iraq. *Engineering and Technology Journal*, **30**(19), 3467-3473.

Abdul Majeed, M.A., Al Naemi, A.N., Al Furaiji, M. and Inmar N. Ghazi, (2022). Fabrication and Characterization of Functionalized Multi-Wall Carbon Nanotubes / Polysulfone Nanocomposite Membranes for Fouling Mitigation. *Int. J. Environment and Waste Management*. DOI: 10.1504/IJEWM.2022.10032160.

Abu-Dalo, M.A., Al-Atoom, M.A., Aljarrah, M.T. and Albiss, B.A. (2022). Preparation and Characterization of Polymer Membranes Impregnated with Carbon Nanotubes for Olive Mill Wastewater. *Polymers*, **14**(3), 457.

Ahmad, N., Souhir, S., Al-Gaashani, R., Muataz, A. A. and Viktor, K. (2019). Antibiofouling Performance by Polyethersulfone Membranes Cast with Oxidized Multiwalled Carbon Nanotubes and Arabic Gum. *Membranes*, **9**(2), 32.

Alalwan, H. A., Augustine, L. J., Hudson, B. G., Abeysinghe, J. P., Gillan, E. G., Mason, S. E., Grassian, V. H. and Cwiertny, D. M. (2021a). Linking Solid-State Reduction Mechanisms to Size-Dependent Reactivity of Metal Oxide Oxygen Carriers for Chemical Looping Combustion. *ACS Applied Energy Materials*, **4**(2), 1163-1172.

Alalwan, H. A., Mohammed, M. M., Sultan, A. J., Abbas, M. N., Ibrahim, T. A., Aljaafari, H. A. and Alminshid, A. A. (2021b). Adsorption of methyl green stain from aqueous solutions using non-conventional adsorbent media: Isothermal kinetic and thermodynamic studies. *Bioresource Technology Reports*, **14**, 100680.

Alhoshan, M., Alam, J., Arockiasamy, L. D. and Al-Homaidi, N. (2013). Fabrication of polysulfone/ZnO membrane: Influence of ZnO nanoparticles on membrane characteristics. Adv. *Polymer Tech.*, **32**(4), 21369-21375.

Alminshid, A. H., Abbas, M. N., Alalwan, H. A., Sultan, A. J., Kadhom, M. A. (2021). Aldol condensation reaction of acetone on MgO nanoparticles surface: An *in-situ* drift investigation. *Molecular Catalysis*, **501**, 111333.

Celik, E., Park, H. and Choi, H. (2011). Carbon nanotube blended polyethersulfone membranes for fouling control in water treatment. *Water Research*, **45**(1), 274-282.

Chandrashekhar, M. N., Inamuddin, A. I., Lakshmi, B. Marwani, H.M., Khan, I. (2020). Polyphenylsulfone/multiwalled carbon nanotubes mixed ultrafiltration membranes: Fabrication, characterization and removal of heavy metals Pb2+, Hg2+, and Cd2+ from aqueous solutions, *Arabian Journal of Chemistry*, **13**(3), 4661-4672.

Choi, Jae-H., Jegal, J. and Kim, W. N. (2007). Modification of Performances of Various Membranes Using MWNTs as a Modifier. *Macromolecular Symposia*, **249-250**(1), 610-617.

Dixon, M. A., Abbas, T., R., Al-Furaiji, M.H. and Abed-Ali, R. H. (2020). Membrane Bioreactor with External Side-Stream Membranes and High Cross Flow Velocity to Treat Municipal Wastewater.

Engineering and Technology Journal, **38**(1), 1-8.
Eman, A. Mwafya, Dawya, M., Abouelsayed, A., Elsabbaghc, I. A. and Elfassc, M. M. (2016). Synthesis and Characterization of Multi-Walled Carbon Nanotubes Decorated ZnO Nanocomposite. *Egypt. J. Chem.,* **59**(6), 1061-1068.
Hossein, M. D., Hua, D. and Chung, Tai-S. (2018). Cross-linked mixed matrix membranes (MMMs) consisting of amine functionalized multi-walled carbon nanotubes and P84 polyimide for organic solvent nanofiltration (OSN) with enhanced flux. *Journal of Membrane Science***, 548**(15), 319-331.
Jiang, X., Cao, Z., Zhang, Yuan, Z., Zimo, L., Xu, X. and Wang, X. (2018). A review of functionalized carbon nanotubes and graphene for heavymetal adsorption from water: Preparation, application, and mechanism. *Chemosphere*, **195**, 351-364.
Jing, C., Xue-Li Cao, Yi, Zhao, Fu-Yi Zhou, Zhaoliang, Cui, Yong, W. and Shi-Peng S. (2020). The establishment of high-performance anti-fouling nanofiltration membranes via cooperation of annular supramolecular Cucurbituril and dendritic polyamidoamine. *Journal of Membrane Science*, **600**, 117863.
Jun, Y., Guocheng, Z. and Baolin D. (2013). Multi-walled carbon nanotubes (MWNTs) / polysulfone (PSU) mixed matrix hollow fiber membranes for enhanced water treatment. *Journal of Membrane Science*, **437**, 237-248.
Kadhom, M., Albayati, N., Salih, S., Al-Furaiji, M., Bayati, M. and Deng, B. (2019b). Role of Cellulose Micro and Nano Crystals in Thin Film and Support Layer of Nanocomposite Membranes for BrackishWater Desalination. *Membranes*, **9**(8), 101.
Kadhom, M. and Deng B. (2019a). Thin film nanocomposite membranes filled with bentonite nanoparticles for brackish water desalination: A novel water uptake concept. *Microporous and Mesoporous Materials***, 279**, 82-91.
Kadhom, M., Yin, J. and Deng, B. (2016). A Thin Film Nanocomposite Membrane with MCM-41
Silica Nanoparticles for Brackish Water Purification. *Membranes (Basel)*, **6**(4), 50.
Kalra, A., Garde S. and Hummer G. (2003, July). Osmotic water transport through carbon nanotube membranes. *Proceedings of the National Academy of Sciences of the United States of America*, **100**(18)10175-10180.
Lalia, B.S., Kochkodan, V., Hashaikeh, R. and Hilal, N. (2013). A review on membrane fabrication: Structure, properties and performance relationship. *Desalination*, **326**, 77–95.
Ma, H., Yoon, K., Rong, L., Shokralla, M., Kopot, A., Wang, X., Fang, D., Hsiao, B.S., B. and Chu, B. (2010). Thin-film nanofibrous composite ultrafiltration membranes based on polyvinyl alcohol barrier layer containing directional water channels. *Industrial & Engineering Chemistry Research*, **49**(23), 11978-84.
Malik, M.M., Nisreen, S. M. A., Alalwan, H. A., Alminshid, A. H. and Aljaafari, H. A.S. (2021). Synthesis of ZnO-CoO/Al2O3 nanoparticles and its application as a catalyst in ethanol conversion to acetone. *Results in Chemistry*, **3**, 100249.
Mansourpanah, Y., Madaeni, S.S., Rahimpour, A., Adeli, M., Hashemi, M.Y. and Moradian, M.R. (2011). Fabrication new PES-based mixed matrix nanocomposite membranes using polycaprolactone modified carbon nanotubes as the additive: Property changes and morphological studies. *Desalination*, **277**(1–3), 171-177.
Narang J. and Chandra S. P. (Eds.) (2018). Current and Future Developments in Nanomaterials and Carbon Nanotubes. *Bentham Science publishers*. (Sharjah, UAE).
Nisreen, S. M. Ali., Alalwan, H. A., Alminshid, A. H. and Malik M. Mohammed. (2022). Synthesis and Characterization of Fe3O4- SiO2 Nanoparticles as Adsorbent Material for Methyl Blue Dye Removal from Aqueous Solutions. *Pollution*, **8**(1), 295-302.
Reyhan, S. Tasdemir, Venkata, R.S.S. M., Derya Y. K. and Ismail K. (2018). Effect of polymer type on characterisation and filtration performances of multiwalled carbon nanotubes (MWCNT)-COOH based polymeric mixed matrix membranes. *Environmental Technology*, **39**(10), 1226-1237.
Waisi, B., Karim, U., Augustijn, D., Al-Furaiji, M., and Hulscher, S. (2015). A study on the quantities and potential use of produced water in southern Iraq. *Water science and technology: water supply*, **15**(2), 370-376.
Weibin, H., Xiaohong, H., Yun, B., Zheng, Li., Yiguo, H., Wang, P., Xiaobo, L. and Kun, J. (2020). Synthesis and self-assembly of polyethersulfone-based amphiphilic block copolymers as microparticles for

suspension immunosensors. *Polymer Chemistry*, **11**(8), 1496-1503

Yalei, Z., Jing, Z., Huaqiang, C., Xuefei, Z. and Yong,W. (2014). Effect of modified attapulgite addition on the performance of a PVDF ultrafiltration membrane. *Desalination*, **344**, 71-78

Zinadini, S., Rostami, S., Vatanpour, V. and Jalilian, E. (2017). Preparation of antibiofouling polyethersulfone mixed matrix NF membrane using photocatalytic activity of ZnO/MWCNTs nanocomposite. *Journal of Membrane Science*, **529**, 133-141.